

# Quantum dynamics of optical phonons generated by optical excitation of a quantum dot: A Wigner function analysis

Daniel Wigger,<sup>1</sup> Helge Gehring,<sup>1</sup> V. Martin Axt,<sup>2</sup> Doris E. Reiter,<sup>1</sup> and Tilmann Kuhn<sup>1</sup>

<sup>1</sup>*Institut für Festkörpertheorie, Universität Münster,  
Wilhelm-Klemm-Str. 10, 48149 Münster, Germany*

<sup>2</sup>*Theoretische Physik III, Universität Bayreuth, 95440 Bayreuth, Germany*  
(Dated: July 18, 2016)

The study of the fundamental properties of phonons is crucial to understand their role in applications in quantum information science, where the active use of phonons is currently highly debated. A genuine quantum phenomenon associated with the fluctuation properties of phonons is squeezing, which is achieved when the fluctuations of a certain variable drop below their respective vacuum value. We consider a semiconductor quantum dot in which the exciton is coupled to phonons. We review the fluctuation properties of the phonons, which are generated by optical manipulation of the quantum dot, in the limiting case of ultra short pulses. Then we discuss the phonon properties for an excitation with finite pulses. Within a generating function formalism we calculate the corresponding fluctuation properties of the phonons and show that phonon squeezing can be achieved by the optical manipulation of the quantum dot exciton for certain conditions even for a single pulse excitation where neither for short nor for long pulses squeezing occurs. To explain the occurrence of squeezing we employ a Wigner function picture providing a detailed understanding of the induced quantum dynamics.

## I. INTRODUCTION

Phonons and their interaction with the electronic degrees of freedom are omnipresent in solid state devices. Typically associated with heat, noise or dissipation, nowadays phonons are becoming actively used, which is the foundation of the emerging field of phononics<sup>1</sup>. Examples are the use of phonons in the form of strain pulses to manipulate the lasing properties of semiconductor structures<sup>2,3</sup> or the application of phonons in the form of surface acoustic waves to control the dynamics in quantum dots<sup>4-8</sup>. The generation of coherent phonons in semiconductor nanostructures has been studied<sup>9,10</sup> and also phonon lasers have been proposed<sup>11</sup>. To explore genuine quantum features of phonons it is interesting to study their fluctuation properties and in particular the emergence of squeezing. Squeezing refers to the reduction of fluctuations of a certain variable below their vacuum level. However, one has to keep in mind that the Heisenberg uncertainty principle has to be fulfilled, which results in increased fluctuations of the conjugate variable. For photons, squeezing is well explored<sup>12-14</sup> and is already used in applications, e.g., to detect gravitational waves at the LIGO experiment<sup>15</sup>. The prospect of finding squeezing also in a mechanical system like phonons, and in particular in semiconductor systems, has triggered a lot of theoretical<sup>16-20</sup> and experimental work<sup>21-24</sup>. In this paper, we will discuss the emergence of squeezing for phonons generated by optically exciting a semiconductor quantum dot.

To be specific, we will study the fluctuation properties of optical phonons which result from an excitation with finite pulses. We will show that the pulse duration is indeed a crucial parameter for phonon squeezing. The theoretical background is introduced in the next Sec. II and the results for various types of excitation conditions

are presented in Sec. III. The paper ends with some concluding remarks in Sec. IV.

## II. THEORY

When searching for non-classical phonon states, it is convenient to use a system, where the electronic part is as simple as possible such that one can focus on the phonon properties. One such system is a self-assembled semiconductor quantum dot (QD) which, under certain conditions, constitutes an electronic two-level system. When the electronic configuration in the QD system changes, in particular by optical excitation with laser light, the lattice reacts to this change by creating phonons. We will show that this can also affect the phonon fluctuations which opens up the possibility to manipulate these fluctuations by changing the excitation conditions.

### A. Model system

In our model we treat the QD as a two-level system, which is justified in the case of a strongly confined QD excited by circularly polarized light, when only excitons with a single spin orientation can be generated. The ground state is denoted by  $|g\rangle$  and the exciton state by  $|x\rangle$ . The states are split by the exciton energy  $\hbar\Omega$ . Taking the energy of the ground state as zero, the system Hamiltonian  $H_{\text{sys}}$  reads

$$H_{\text{sys}} = \hbar\Omega|x\rangle\langle x|. \quad (1)$$

The coupling to the classical light field  $E(t)$  is treated in dipole and rotating wave approximation via the Hamil-

tonian

$$H_{\text{sys-light}} = -M_0 [E^{(-)}(t)|g\rangle\langle x| + E^{(+)}(t)|x\rangle\langle g|] , \quad (2)$$

where  $M_0$  is the dipole matrix element and

$$E^{(\pm)}(t) = \frac{\hbar\Omega_R(t)}{2M_0} e^{\mp i\omega_L t} \quad (3)$$

are the positive (upper sign) and negative (lower sign) frequency component of the electric field of the laser pulse with central frequency  $\omega_L$ . Here we have expressed the pulse shape in terms of the instantaneous Rabi frequency  $\Omega_R$ . Both the dipole matrix element and the Rabi frequency are taken to be real and we assume a Gaussian envelope with

$$\Omega_R(t) = \frac{\Theta}{\tau\sqrt{2\pi}} \exp\left[-\frac{(t-t_0)^2}{2\tau^2}\right] . \quad (4)$$

The pulse duration is determined by  $\tau$  and  $\Theta$  denotes the pulse area, which is defined such that in the absence of phonons a resonant  $\pi$  pulse (i.e., a pulse with  $\Theta = \pi$ ) completely excites the exciton from the ground state.

In addition, we take into account the electron-phonon interaction. The phonon Hamiltonian is given by

$$H_{\text{pho}} = \sum_{\mathbf{q}} [\hbar\omega_{\mathbf{q}} b_{\mathbf{q}}^\dagger b_{\mathbf{q}} + \hbar g_{\mathbf{q}} (b_{\mathbf{q}}^\dagger + b_{\mathbf{q}}) |x\rangle\langle x|] , \quad (5)$$

where  $b_{\mathbf{q}}^\dagger$  ( $b_{\mathbf{q}}$ ) are the creation (annihilation) operators for a phonon. For simplicity we assume that, as in the case of bulk phonons, the phonons can be classified in terms of a wave vector  $\mathbf{q}$ . A generalization to arbitrary phonon quantum numbers is straightforward. The first part in Eq. (5) describes the free phonon part with the dispersion relation  $\omega_{\mathbf{q}}$  and the second term describes the pure dephasing-type carrier-phonon interaction via the coupling matrix element  $g_{\mathbf{q}}$ . The Hamiltonian Eq. (5) describes the fact that, due to the large difference between exciton and phonon energy the phonons do not induce transitions between exciton and ground state. They affect, however, the phase of the coherence between these states which, for finite pulses, also has an influence on the resulting occupation. In general, there can be different types of phonon modes (e.g., acoustic and optical, longitudinal and transverse) and different coupling mechanisms (e.g., deformation potential or polar). Here we assume that all these can be treated separately.

The operators for the phonon displacement  $\mathbf{u} = \langle \hat{\mathbf{u}} \rangle$  and phonon momentum  $\boldsymbol{\pi} = \langle \hat{\boldsymbol{\pi}} \rangle$  are related to the phonon mode operators  $b_{\mathbf{q}}$  and  $b_{\mathbf{q}}^\dagger$  via

$$\hat{\mathbf{u}}(\mathbf{r}) = i \sum_{\mathbf{q}} \sqrt{\frac{\hbar}{2\varrho V \omega_{\mathbf{q}}}} \mathbf{e}_{\mathbf{q}} (b_{\mathbf{q}} + b_{-\mathbf{q}}^\dagger) e^{i\mathbf{q}\cdot\mathbf{r}} \quad (6a)$$

and

$$\hat{\boldsymbol{\pi}}(\mathbf{r}) = \sum_{\mathbf{q}} \sqrt{\frac{\varrho \hbar \omega_{\mathbf{q}}}{2V}} \mathbf{e}_{\mathbf{q}} (b_{\mathbf{q}} - b_{-\mathbf{q}}^\dagger) e^{i\mathbf{q}\cdot\mathbf{r}} , \quad (6b)$$

where  $\mathbf{e}_{\mathbf{q}}$  denotes the polarization vector of the phonon mode,  $\varrho$  is the crystal density and  $V$  is the normalization volume. In this paper, we are particularly interested in the fluctuation properties of the phonon displacement and momentum. These are given by

$$(\Delta \mathbf{u})^2 = \langle \hat{\mathbf{u}}^2 \rangle - \langle \hat{\mathbf{u}} \rangle^2 \quad \text{and} \quad (\Delta \boldsymbol{\pi})^2 = \langle \hat{\boldsymbol{\pi}}^2 \rangle - \langle \hat{\boldsymbol{\pi}} \rangle^2 . \quad (7)$$

Squeezing occurs, if the fluctuations fall below their respective vacuum value  $(\Delta \mathbf{u})_{\text{vac}}^2$  and  $(\Delta \boldsymbol{\pi})_{\text{vac}}^2$ . To simplify the discussion, we introduce the quantities

$$D_u = \frac{(\Delta \mathbf{u})^2 - (\Delta \mathbf{u})_{\text{vac}}^2}{(\Delta \mathbf{u})_{\text{vac}}^2} \quad (8a)$$

and

$$D_\pi = \frac{(\Delta \boldsymbol{\pi})^2 - (\Delta \boldsymbol{\pi})_{\text{vac}}^2}{(\Delta \boldsymbol{\pi})_{\text{vac}}^2} . \quad (8b)$$

These definitions are particularly handy to identify squeezing, because we only need to check if these quantities, which for simplicity we will call fluctuations in the following, become negative. Thus, the presence of displacement or momentum squeezing is equivalent to  $D_u < 0$  or  $D_\pi < 0$ , respectively.

## B. Generating function formalism

To calculate the dynamics of the system, we use generating functions which are defined as the expectation values<sup>25,26</sup>

$$\rho_{\nu\nu'}(\{\alpha_{\mathbf{q}}\}, \{\beta_{\mathbf{q}}\}) = \langle |\nu\rangle \langle \nu'| e^{\sum_{\mathbf{q}} \alpha_{\mathbf{q}} b_{\mathbf{q}}^\dagger} e^{\sum_{\mathbf{q}} \beta_{\mathbf{q}} b_{\mathbf{q}}} \rangle . \quad (9)$$

Here,  $|\nu\rangle$  denotes the electronic state of the system, i.e.,  $|\nu\rangle \in \{|g\rangle, |x\rangle\}$  and  $\alpha_{\mathbf{q}}, \beta_{\mathbf{q}}$  are complex numbers. From the generating functions, all electronic and phononic variables can be calculated. The pure phonon variables are encoded in the function

$$\begin{aligned} F(\{\alpha_{\mathbf{q}}\}, \{\beta_{\mathbf{q}}\}) &= \langle e^{\sum_{\mathbf{q}} \alpha_{\mathbf{q}} b_{\mathbf{q}}^\dagger} e^{\sum_{\mathbf{q}} \beta_{\mathbf{q}} b_{\mathbf{q}}} \rangle \\ &= \sum_{\nu} \rho_{\nu\nu}(\{\alpha_{\mathbf{q}}\}, \{\beta_{\mathbf{q}}\}) , \end{aligned} \quad (10a)$$

while the quantities related to the occupation of the electronic levels are given by the function  $C$  and those related to the interband coherence are encoded in the function  $Y$  with

$$Y(\{\alpha_{\mathbf{q}}\}, \{\beta_{\mathbf{q}}\}) = \langle |g\rangle \langle x| e^{\sum_{\mathbf{q}} \alpha_{\mathbf{q}} b_{\mathbf{q}}^\dagger} e^{\sum_{\mathbf{q}} \beta_{\mathbf{q}} b_{\mathbf{q}}} \rangle , \quad (10b)$$

$$C(\{\alpha_{\mathbf{q}}\}, \{\beta_{\mathbf{q}}\}) = \langle |x\rangle \langle x| e^{\sum_{\mathbf{q}} \alpha_{\mathbf{q}} b_{\mathbf{q}}^\dagger} e^{\sum_{\mathbf{q}} \beta_{\mathbf{q}} b_{\mathbf{q}}} \rangle . \quad (10c)$$

For example, for  $\{\alpha_{\mathbf{q}}\} = \{\beta_{\mathbf{q}}\} = 0$ , we retain the occupation  $f = \langle |x\rangle \langle x| \rangle = C(0, 0)$ , while phononic and phonon assisted variables can be obtained by derivatives of the

corresponding functions with respect to  $\alpha_{\mathbf{q}}$  and  $\beta_{\mathbf{q}}$  and setting  $\{\alpha_{\mathbf{q}}\} = \{\beta_{\mathbf{q}}\} = 0$  afterwards, such as

$$\langle b_{\mathbf{q}} \rangle = \frac{\partial}{\partial \beta_{\mathbf{q}}} F(\{\alpha_{\mathbf{q}}\}, \{\beta_{\mathbf{q}}\}) \Big|_{\{\alpha_{\mathbf{q}}\}=\{\beta_{\mathbf{q}}\}=0}, \quad (11a)$$

$$\langle b_{\mathbf{q}}^\dagger b_{\mathbf{q}} \rangle = \frac{\partial^2}{\partial \beta_{\mathbf{q}} \partial \alpha_{\mathbf{q}}} F(\{\alpha_{\mathbf{q}}\}, \{\beta_{\mathbf{q}}\}) \Big|_{\{\alpha_{\mathbf{q}}\}=\{\beta_{\mathbf{q}}\}=0}. \quad (11b)$$

Using Heisenberg's equations of motion, a closed set of equations of motion for the generating functions  $F$ ,  $Y$ , and  $C$  can be derived<sup>25</sup>. These are partial differential equations containing derivatives with respect to  $t$ ,  $\alpha_{\mathbf{q}}$ , and  $\beta_{\mathbf{q}}$ . It has been shown that for an excitation with an arbitrary series of ultra short pulses an analytical solution of these equations of motion can be found, which holds for any type of dispersion relation  $\omega_{\mathbf{q}}$  and coupling matrix element  $g_{\mathbf{q}}$  and thus both for optical and acoustic phonons<sup>25,26</sup>. The limit of ultra short pulses is reached when the pulse duration is much shorter than the characteristic phonon-induced time scale. In this case the light-induced dynamics during the pulses and the phonon-induced dynamics between and after the pulses can be separated. For longer pulses, when this separation of time scales is not anymore fulfilled, no analytical solution is known and numerical techniques have to be applied. In the following we will concentrate on the case of interaction with optical phonons, in which a numerically tractable set of equations of motion for the characteristic functions can be obtained. A detailed discussion of the phonon dynamics and phonon squeezing in the case of acoustic phonons can be found in Refs.<sup>27-29</sup>. For acoustic phonons it has been found that squeezed single or sequences of wave packets can be generated, which travel away from the QD with the speed of sound.

### C. Coupling to optical phonons

Optical phonons are typically characterized by a negligible dispersion over the range of wave vectors which are coupled to the QD exciton. Thus, they are well approximated by a constant phonon frequency  $\omega_{\text{LO}}$ . Due to their vanishing group velocity, optical phonons do not travel but stay confined to the QD region where they are generated. Typically, longitudinal optical (LO) phonons are much more strongly coupled to the QD exciton than transverse optical (TO) phonons. Therefore in the following we will refer to LO phonons, although the formalism is the same for TO phonons.

In the case of a constant phonon frequency it is possible to rewrite the phonon modes in such a form that only a small number of modes couples to the exciton<sup>30</sup>. We call the annihilation and creation operators in the new basis  $B_\lambda$  and  $B_\lambda^\dagger$ . For an  $N$ -level system, at most  $N(N+1)/2$  modes are coupled<sup>30</sup>, which in the case of a two-level system evaluates to three modes. Because we take into account only the pure dephasing mechanism only the coupling matrix element to the excited state is

non-zero. Therefore, we can further reduce the number of coupled modes to a single one with the coupling strength  $G = \sqrt{\sum_{\mathbf{q}} |g_{\mathbf{q}}|^2}$ <sup>31</sup>. We further define the dimensionless coupling  $\Gamma = G/\omega_{\text{LO}}$ . The ladder operators of the coupled mode are then given by

$$B_0 = \sum_{\mathbf{q}} \frac{g_{\mathbf{q}}}{G} b_{\mathbf{q}} \quad \text{and} \quad B_0^\dagger = \sum_{\mathbf{q}} \frac{g_{\mathbf{q}}}{G} b_{\mathbf{q}}^\dagger. \quad (12)$$

The other modes with  $\lambda \neq 0$  are taken to be orthogonal to the coupled one. With this, the phonon Hamiltonian reads

$$H_{\text{pho}} = \hbar \omega_{\text{LO}} \sum_{\lambda} B_\lambda^\dagger B_\lambda + \hbar G (B_0^\dagger + B_0) |x\rangle \langle x|. \quad (13)$$

To describe the coupled exciton-phonon dynamics for this system the generating functions can be reduced to the single-mode case with only a single pair of variables  $\alpha$  and  $\beta$  according to

$$F(\alpha, \beta) = \langle e^{\alpha B_0^\dagger} e^{\beta B_0} \rangle, \quad (14a)$$

$$Y(\alpha, \beta) = \langle |g\rangle \langle x| e^{\alpha B_0^\dagger} e^{\beta B_0} \rangle, \quad (14b)$$

$$C(\alpha, \beta) = \langle |x\rangle \langle x| e^{\alpha B_0^\dagger} e^{\beta B_0} \rangle. \quad (14c)$$

These generating functions satisfy the closed set of equations

$$i\partial_t F = \omega_{\text{LO}} [\beta \partial_\beta - \alpha \partial_\alpha] F + G [\beta - \alpha] C, \quad (15a)$$

$$i\partial_t Y = [\Omega + \omega_{\text{LO}} (\beta \partial_\beta - \alpha \partial_\alpha) + G (\beta + \partial_\alpha + \partial_\beta)] Y - \frac{1}{2} \Omega_{\text{R}}(t) [F - 2C] e^{-i\omega_{\text{L}} t}, \quad (15b)$$

$$i\partial_t C = [\omega_{\text{LO}} (\beta \partial_\beta - \alpha \partial_\alpha) + G (\beta - \alpha)] C - \frac{1}{2} \Omega_{\text{R}}(t) [Y^T e^{-i\omega_{\text{L}} t} - Y e^{i\omega_{\text{L}} t}], \quad (15c)$$

with  $Y^T(\alpha, \beta) = Y^*(\beta^*, \alpha^*)$ . To further simplify these equations, we transform the system into a rotating frame on the polaron shifted excitation frequency  $\bar{\omega}_{\text{L}} = \omega_{\text{L}} - \omega_{\text{LO}} \Gamma^2$  resulting in the new variables

$$\bar{F}(\alpha, \beta) = F(\alpha e^{-i\omega_{\text{LO}} t}, \beta e^{i\omega_{\text{LO}} t}), \quad (16a)$$

$$\bar{Y}(\alpha, \beta) = \exp[i\bar{\omega}_{\text{L}} t + \beta \Gamma e^{i\omega_{\text{LO}} t}] \times Y(\alpha e^{-i\omega_{\text{LO}} t} + \Gamma, \beta e^{i\omega_{\text{LO}} t} - \Gamma), \quad (16b)$$

$$\bar{C}(\alpha, \beta) = \exp[\Gamma (\beta e^{i\omega_{\text{LO}} t} + \alpha e^{-i\omega_{\text{LO}} t})] \times C(\alpha e^{-i\omega_{\text{LO}} t}, \beta e^{i\omega_{\text{LO}} t}) \quad (16c)$$

and

$$\bar{\Omega}_{\text{R}} = \Omega_{\text{R}} e^{i(\bar{\omega}_{\text{L}} - \omega_{\text{L}}) t}. \quad (16d)$$

The notation can be further simplified by noticing that for the calculation of the relevant expectation values  $\alpha$  and  $\beta$  are not independent, instead it is sufficient to calculate the functions  $\bar{f}(\alpha, t) = \bar{f}(-\alpha^*, \alpha, t)$  where  $\bar{f}$  stands

for  $\bar{F}$ ,  $\bar{Y}$  and  $\bar{C}$ , respectively. The resulting equations of motion in the case of resonant excitation read

$$\partial_t \bar{F}(\alpha) = -2i\omega_{\text{LO}} \Gamma \text{Re}(\alpha e^{i\omega_{\text{LO}} t}) \times \exp[-2i\Gamma \text{Im}(\alpha e^{i\omega_{\text{LO}} t})] \bar{C}(\alpha), \quad (17a)$$

$$\partial_t \bar{Y}(\alpha) = \frac{i}{2} \bar{\Omega}_{\text{R}} \left[ e^{\alpha \Gamma e^{i\omega_{\text{LO}} t}} \bar{F}(\alpha - \Gamma e^{-i\omega_{\text{LO}} t}) - 2e^{\alpha^* \Gamma e^{-i\omega_{\text{LO}} t}} \bar{C}(\alpha - \Gamma e^{-i\omega_{\text{LO}} t}) \right], \quad (17b)$$

$$\partial_t \bar{C}(\alpha) = \frac{i}{2} e^{-\Gamma^2} \left[ \bar{\Omega}_{\text{R}} e^{\alpha \Gamma e^{i\omega_{\text{LO}} t}} \bar{Y}^*(\Gamma e^{-i\omega_{\text{LO}} t} - \alpha) - \bar{\Omega}_{\text{R}}^* e^{-\alpha^* \Gamma e^{-i\omega_{\text{LO}} t}} \bar{Y}(\Gamma e^{-i\omega_{\text{LO}} t} + \alpha) \right] \quad (17c)$$

For the excitation with ultra short pulses, described mathematically in terms of  $\delta$ -functions, an analytical solution of these equations can be found<sup>25,26,32</sup>, while in the case of extended pulses, the equations cannot be solved analytically anymore. Instead, a numerical integration of the equations of motion is needed<sup>32</sup>, which is feasible here since the infinite number of variables  $\alpha_{\mathbf{q}}$ ,  $\beta_{\mathbf{q}}$  in the multi-mode case has been reduced to a single complex variable  $\alpha$ . However, due to the shifted arguments on the right hand side of Eq. (17) all  $\alpha$ -values are coupled. For the numerical integration we have used a standard fourth-order Runge-Kutta method. The initial conditions were chosen such that the system is initially in the ground state at temperature  $T = 0$  K resulting in  $\bar{C}(t=0) = \bar{Y}(t=0) = 0$  and  $\bar{F}(t=0) = 1$ .

Having introduced a single LO phonon mode, it is possible to describe the state of the LO phonons in terms of a Wigner function in the phase space spanned by variables  $U$  and  $\Pi$ <sup>33</sup>.  $U$  and  $\Pi$  are the phase space representations of the corresponding operators  $\hat{U}$  and  $\hat{\Pi}$ , which are directly connected to the phonon creation and annihilation operators of the coupled mode via

$$\hat{U} = B_0 + B_0^\dagger \quad \text{and} \quad \hat{\Pi} = i(B_0 - B_0^\dagger). \quad (18)$$

For simplicity, although defined in a dimensionless form, we will refer to  $U$  as displacement and  $\Pi$  as momentum in the following.

The Wigner function is the quantum mechanical analogue of a phase-space distribution function. It is a real-valued function, however, in contrast to a classical distribution function the Wigner function can become negative. Negative values of the Wigner function therefore indicate genuine quantum mechanical behavior. From the generating phonon function the Wigner function is calculated via the characteristic Wigner function<sup>33</sup>

$$C_W(\alpha) = \left\langle e^{\alpha B_0^\dagger - \alpha^* B_0} \right\rangle = e^{-\frac{1}{2}|\alpha|^2} \left\langle e^{\alpha B_0^\dagger} e^{-\alpha^* B_0} \right\rangle = e^{-\frac{1}{2}|\alpha|^2} F(\alpha, -\alpha^*). \quad (19)$$

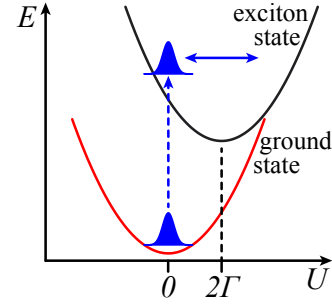


Figure 1. Sketch of the phonon potential for the ground state and the exciton state. The phonon states are marked by the blue envelopes.

With this, the Wigner function is

$$\begin{aligned} W(z) &= \frac{1}{\pi^2} \iint e^{\alpha^* z - \alpha z^*} C_W(\alpha) d^2 \alpha \\ &= \frac{1}{\pi^2} \iint e^{\alpha^* z - \alpha z^*} e^{-\frac{1}{2}|\alpha|^2} F(\alpha, -\alpha^*) d^2 \alpha \\ &= \frac{1}{\pi^2} \iint e^{\alpha^* z e^{-i\omega_{\text{LO}} t} - \alpha z^* e^{i\omega_{\text{LO}} t} - \frac{1}{2}|\alpha|^2} \bar{F}(-\alpha^*) d^2 \alpha. \end{aligned} \quad (20)$$

Here,  $z$  is a complex number and we define  $\text{Re}(z) = \frac{U}{2}$  and  $\text{Im}(z) = -\frac{\Pi}{2}$ . Non-negative probability distributions  $P(U)$  and  $P(\Pi)$  can be obtained from the Wigner function by integration over  $\Pi$  and  $U$ , respectively. From these probability distributions expectation values and fluctuations can be calculated in the standard way such as, e.g., for the operator  $\hat{U}$ :

$$\langle \hat{U} \rangle = \int U P(U) dU = \iint U W(U, \Pi) d\Pi dU \quad (21a)$$

$$\langle \hat{U}^2 \rangle = \int U^2 P(U) dU. \quad (21b)$$

Likewise, scaled fluctuations are introduced according to

$$D_U = \frac{(\Delta U)^2 - (\Delta U)_{\text{vac}}^2}{(\Delta U)_{\text{vac}}^2} \quad (22a)$$

and

$$D_\Pi = \frac{(\Delta \Pi)^2 - (\Delta \Pi)_{\text{vac}}^2}{(\Delta \Pi)_{\text{vac}}^2}. \quad (22b)$$

Correspondingly, the phonon state is squeezed, when either  $D_U < 0$  or  $D_\Pi < 0$ .

### III. RESULTS

In the following we will discuss the phonon dynamics and in particular the possibility to achieve phonon squeezing for different excitation conditions. We will start by discussing the limiting cases of pulses which are very short or very long compared to the inverse of the

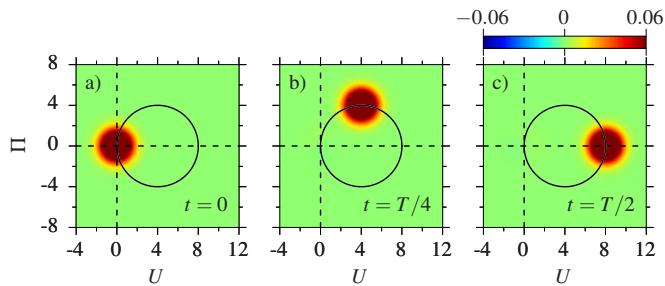


Figure 2. Snapshots of the LO phonon Wigner function for a  $\pi$  pulse excitation with an ultra short pulse ( $\tau \ll T$ ) at three different times.

phonon frequency. Then we will come to the case of comparable time scales of the light-induced and phonon-induced dynamics.

To be specific, we consider the case of a GaAs-type QD coupled via the Fröhlich interaction to bulk LO phonons with an energy of  $\hbar\omega_{\text{LO}} = 36.4$  meV, such that the phonon period is  $T = 2\pi/\omega_{\text{LO}} = 114$  fs. The typical coupling strength in such dots is rather weak with about  $\Gamma = 0.03$ , but can be enhanced via charge separation by applying an external electric field up to  $\Gamma = 0.8$ <sup>31</sup>. To facilitate the interpretation of the results, in the case of ultra short and ultra long pulses we have used an increased value of  $\Gamma = 2$ , which could be realized in more polar materials. A comparison with values more typical for GaAs-type QDs can be found in<sup>31</sup>.

### A. Ultra short pulses

The phonon dynamics induced by a single or a pair of ultra short optical pulses has been analyzed in detail in Refs.<sup>18,31</sup>. Here we review the main results, which serve as a reference for the case of longer pulses discussed below.

Before discussing the generation of squeezed phonons, it is instructive to recall some features of coherent phonons. Coherent states fulfill the Heisenberg uncertainty relation between the fluctuations of the displacement  $\Delta U$  and the fluctuations of the momentum  $\Delta \Pi$  at its minimum value. Furthermore, in the dimensionless form of  $U$  and  $\Pi$  introduced above both fluctuations are equal. This condition is also realized, when the fluctuations agree with their vacuum values. In this sense, the vacuum state is a specific coherent state. Since phonons are described by bosonic ladder operators in the harmonic approximation, the vacuum state can be described by the ground state in a harmonic potential as sketched in Fig. 1. Phonons are in the vacuum state, when no phonon excitation has taken place, and in particular, when the QD is in its ground state prior to the optical excitation. In terms of the Wigner function, the vacuum state corresponds to a two-dimensional Gaussian with equal widths in  $U$  and  $\Pi$ , which is centered at the origin as displayed

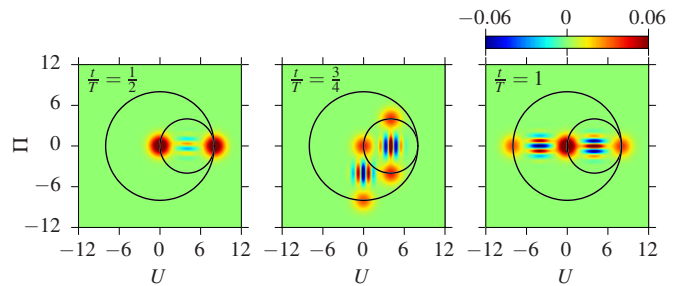


Figure 3. Snapshots of the LO phonon Wigner function for an excitation with two ultra short  $\pi/2$  pulses with a delay of  $T/2$  between them leading to the formation of two cat states.

in Fig. 2 a). If the QD exciton is created, e.g., by the application of a  $\pi$  pulse, the harmonic potential for the phonons shifts due to the electron-phonon interaction, thus the equilibrium position for the phonons associated with the exciton state lies at a finite value of  $U$ , which is determined by the coupling constant  $\Gamma$ . This is illustrated in Fig. 1. In the limiting case of an ultra short pulse, the optical excitation occurs so fast that the lattice ions cannot follow. Thus, the potential changes instantaneously while the form and position of the wave function are conserved. In the shifted potential, the state is now displaced with respect to the potential minimum at  $U = 2\Gamma$  making it a coherent state, which oscillates in time<sup>18,25,34</sup>. In the Wigner function for the LO phonons shown in Fig. 2 a)-c) at three different times this is clearly visible. The Wigner function moves on a circle around its new equilibrium position at  $(2\Gamma, 0)$ , but keeps its form. We want to remark that here the value of the coupling constant  $\Gamma$  only determines the position of the shifted equilibrium. The subsequent dynamics is not affected by this value.

Let us now turn to squeezed phonons. In the Wigner function, squeezing is seen, when the phase space distribution looks indeed squeezed, i.e., it is narrower in one direction in phase space than the Wigner function of the coherent state, hence its name. There are several ways to create squeezed states. Typically squeezing is described by the action of the a squeezing operator on a coherent state<sup>35</sup>, but also special superposition states can lead to squeezing. In the Wigner function quantum mechanical effects are indicated by negative values, which can result in a reduced width. In a more strict definition, squeezing occurs, if the fluctuations of one of the variables fall below their respective vacuum fluctuations. Because of the Heisenberg uncertainty principle this always results in an increased fluctuation of the other variable and, thus, a squeezed Wigner function.

The optical excitation by a single ultra short pulse only results in a coherent state or, if the optical excitation is not complete, in a statistical mixture of vacuum state and coherent state. Thus, squeezing is never achieved in this case. However, using two ultra short pulses it has been shown that it is possible to excite squeezed phonon

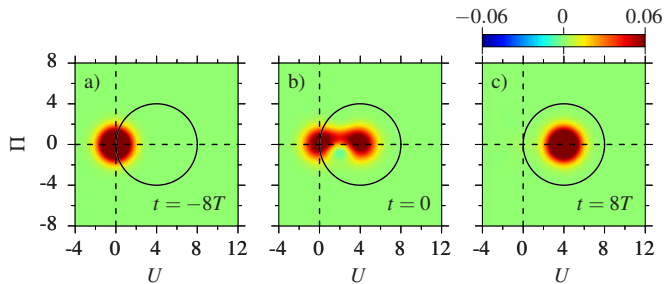


Figure 4. Snapshots of the LO phonon Wigner function for a  $\pi$  pulse excitation with an ultra long pulse ( $\tau \gg T$ ) at three different times.

states<sup>18,31</sup>. The occurrence of squeezing can be explained by the build up of phononic cat states<sup>31</sup>, which are superpositions of two coherent states. One example of the phonon Wigner function for the excitation with two  $\pi/2$  pulses with a delay of  $T/2$  is shown in Fig. 3. The two circles represent the movement of the centers of the coherent states, where the smaller circle corresponds to the exciton potential and the larger one to the ground state potential. For certain parameters squeezing occurs in cat states due to the quantum mechanical interference<sup>36</sup>, when the states are close enough to overlap in phase space. In Ref.<sup>31</sup> we have shown that squeezing for a two pulse excitation can be found for a wide range of parameters considering coupling strength, phase relation between the pulses, delay and pulse areas.

### B. Ultra long pulses

In the other limiting case of a pulse that is very long compared to the phonon period, the situation is different. The corresponding Wigner function is shown again at three different times in Fig. 4 a)-c). In this case no analytical solution is possible, instead the Wigner function has been obtained from the numerical solution of the equations of motion [Eq. (17)] for the generating functions. During the pulse the phonons are in a mixture of the phonon ground states associated with the two electronic potentials. Thus, the Wigner function changes its shape as seen in Fig. 4 b), eventually reaching its new equilibrium depicted in Fig. 4 c), as is expected for a quasi-adiabatic state preparation of the exciton. This new equilibrium state represents the polaron that has been built up. The final state after the pulse is therefore again a symmetric Gaussian, but now at the new equilibrium position ( $2\Gamma, 0$ ). In the exciton subsystem it is the vacuum state, while seen from the perspective of the electronic ground state it is displaced and thus a coherent but stationary state. Again this does not alter the fluctuation properties of the phonons.

In Ref.<sup>34</sup> it was reported that the action of a long pulse

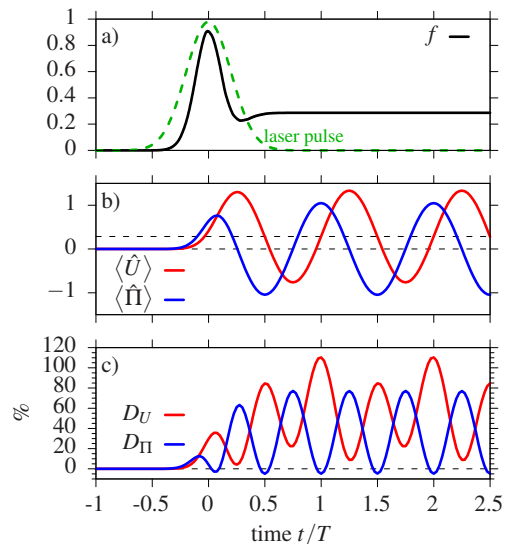


Figure 5. a) Occupation of the exciton state  $f$  and laser pulse, b) expectation values of the displacement  $\langle \hat{U} \rangle$  and of the momentum  $\langle \hat{\Pi} \rangle$  and c) their fluctuations.

would result in the creation of a Fock state, which is in contrast to our findings. We attribute this discrepancy to the use of perturbation theory in Ref.<sup>34</sup>, which might lose its validity in the limit of long times. Note that our generating function treatment provides a numerically complete solution of the dynamics in the considered model without further approximation except for the discretization of  $t$  and  $\alpha$ , which is however well controlled. In particular, no perturbative approximation is made. Indeed, for the short pulse excitation, where perturbation theory typically works properly, our results and the results found in Ref.<sup>34</sup> agree on the creation of a coherent state.

From our calculations we thus conclude that both excitations with ultra short and ultra long single pulses yield coherent phonon states after the excitation<sup>18,31</sup>, in the former case oscillating around the new equilibrium position and in the latter case localized at this equilibrium position. Also during the long pulse, the fluctuations remain at or above the vacuum levels, as already implied by the stretched Wigner function in Fig. 4 b).

### C. Pulses with finite duration

We now analyze the case of excitation by pulses with pulse durations in the intermediate regime, i.e., in the regime where the pulse duration  $\tau$  and the phonon oscillation period  $T$  are of the same order. In this section we set  $\Gamma = 0.5$ , which is a reasonable value for a GaAs QD in the presence of an applied electric field.



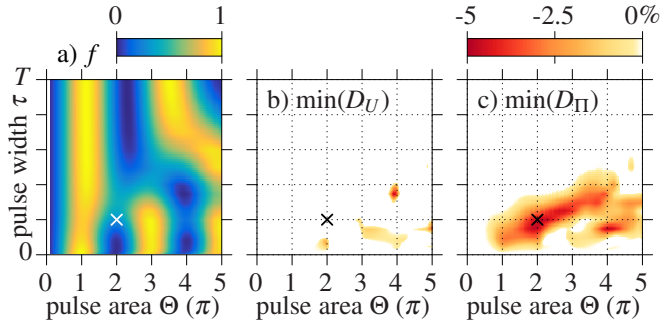


Figure 6. a) Occupation of the excited state, b) minimum of the fluctuations of the displacement and c) minimum of the fluctuations of the momentum. All at times after the pulse and plotted as a function of pulse area  $\Theta$  and pulse width  $\tau$ . Note that the color scale is restricted to negative values for b) and c).

### 1. Single pulse excitation

Figure 5 shows the dynamics of the LO phonon system after the excitation with a single finite pulse with a pulse area of  $\Theta = 2\pi$  and a pulse length of  $\tau = 0.2T$ , which in the case of GaAs corresponds to a pulse with a full width at half maximum (FWHM) of about 50 fs. In Fig. 5 a) the laser pulse and the occupation  $f$  of the exciton state is shown, while in Fig. 5 b) the expectation values of the displacement  $\langle \hat{U} \rangle$  and of the momentum  $\langle \hat{\Pi} \rangle$  are displayed. Figure 5 c) shows the respective fluctuations for these excitation conditions. During the action of the laser pulse, which is from about  $t = -0.5T$  to  $t = 0.5T$ , the occupation cycles once through maximum and minimum, however, due to the phonon interaction, after the pulse an occupation of about  $f = 0.285$  remains in the system. Without the interaction one would expect a final value of  $f = 0$  for a pulse with  $\Theta = 2\pi$ . Likewise the phonon expectation values and fluctuations start to oscillate. The expectation value of the displacement  $\langle \hat{U} \rangle$  oscillates around a shifted mean value. This shift is due to the shifted equilibrium position in the excitonic subsystem ( $2\Gamma$ ), which contributes to the overall mean value weighted by the occupation  $f$ . So  $\langle \hat{U} \rangle$  oscillates around  $f \cdot 2\Gamma = 0.285$ , marked as upper dashed line in Fig. 5 b). The fluctuations  $D_U$  also show a periodic behavior, however, for all times the fluctuations are enhanced, such that a displacement squeezing does not take place. For the momentum, we find that the expectation value of the momentum  $\langle \hat{\Pi} \rangle$  oscillates around 0 and also the fluctuations  $D_\Pi$  oscillate sinusoidal. Here, we see each minimum is below 0 showing the occurrence of momentum squeezing.

To analyze in more detail, whether we can have squeezing for a single pulse excitation, we have performed a systematic analysis of the fluctuations  $D_U$  and  $D_\Pi$  as function of the pulse area  $\Theta$  and the pulse duration  $\tau$ . For this we have extracted the minimal value of  $D_U$  and  $D_\Pi$  after the action of the pulse, e.g., for  $t > 0.5T$  in

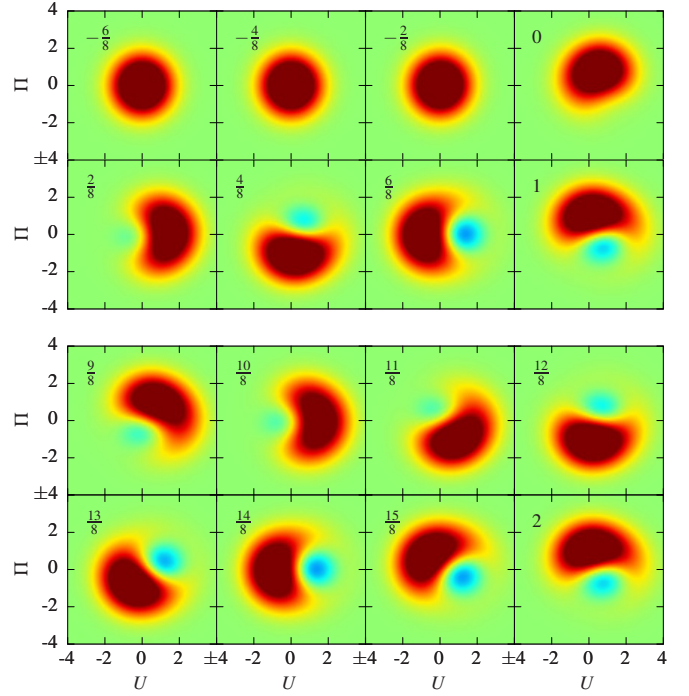


Figure 7. Snapshots of the Wigner function for a  $2\pi$ -pulse with  $\tau = 0.2T$  for different times  $t/T$ .

the previous example. Because we consider LO phonons and we have neglected any phonon decay, the oscillation after the pulse is periodic with the phonon period  $T$  and will go on forever. For very long times, phonon decay processes would eventually destroy the phonon signal in real systems. Furthermore, radiative decay processes would lead to a relaxation from the exciton to the ground state. These processes, however, occur on much longer time scales than considered here.

The results for the minimum values of  $D_U$  and  $D_\Pi$  are shown in Fig. 6 together with the corresponding occupation  $f$  of the exciton state. Note that for  $\min(D_U)$  and  $\min(D_\Pi)$  we only show the negative values for clarity, i.e., it is not shown if the minimum is above zero. For an intermediate pulse length up to  $\tau = 0.5T$  we find that squeezing of both displacement and momentum can indeed occur, however the degree of squeezing is rather small with less than 5%. We find that squeezing occurs in the transition region between the limiting cases of ultra short and long pulses. Interestingly, the occurrence of squeezing is accompanied by a rather atypical behavior of the occupation. While for ultra short pulses we find the typical Rabi rotations with maxima at  $\Theta = (2n+1)\pi$ , for longer pulses, the phonon-induced renormalization of the Rabi rotations is clearly visible, i.e., the period of the Rabi flops gets longer. For intermediate pulse areas no clear Rabi rotations can be identified. When we look at the fluctuations, we find that exactly in the region with intermediate pulse duration, the fluctuations of the phonons fall below their vacuum value, i.e., squeezed states emerge.

To understand the behavior in more detail, we look at the corresponding Wigner function plotted in Fig. 7. During the rise of the pulse up to  $t = 0$  the phonons do not react significantly to the change in the electronic system and essentially stay in the vacuum state. Only around  $t = 0$ , we find that the phonons start to noticeably react to their new potential from the exciton state and move out of the center of phase space. While they start to oscillate, the electronic system already moves back to the ground state. Thus, instead of a coherent state in form of a symmetric Gaussian, a deformed shape is formed. We also find negative values of the Wigner function. This indicates that the phonon state contains features that are of genuine quantum mechanical nature. After the action of the pulse, for  $t > T$ , we see that the Wigner function rotates, but its form is not stable. Around the times  $t = T$  and  $t = 3T/2$ , where the momentum is squeezed, we see that the Wigner function is indeed elongated along  $U$ , but narrow in  $\Pi$ . On the other hand at time  $t = 5T/4$  and  $t = 7T/4$ , where the fluctuations of the displacement have a minimum, the Wigner function is elongated along  $\Pi$ . Though negative parts appear in the Wigner function, it is still wider than in the vacuum case and no squeezing occurs.

Since the QD is driven by a coherent light field and the initial state is a pure state (the ground state of the QD-phonon system), the total system consisting of QD exciton and phonons remains always in a pure state. However, in general the temporal evolution results in an entanglement of the electronic and the phononic subsystem. When only one of the two subsystems is considered, the other system is traced out. This leads to a loss of coherence. If the electronic system is traced out, the phononic system falls apart into two parts: one belonging to the ground state potential and one belonging to the exciton state potential. Due to the loss of coherence, these two parts are in a statistical mixture. Note that each part on its own corresponds to a pure state. Also the Wigner function can be separated into these two parts with  $W_g(U, \Pi)$  being the Wigner function in the ground state potential and  $W_x(U, \Pi)$  for the exciton potential. The total Wigner function is the sum of both parts  $W(U, \Pi) = W_g(U, \Pi) + W_x(U, \Pi)$  reflecting the statistical mixture. One example for this is shown in Fig. 8. For both parts  $W_g(U, \Pi)$  and  $W_x(U, \Pi)$  we find a banana shaped Wigner function consisting of a positive region that bends around a negative one. Each part now rotates with a stable shape around its respective equilibrium, i.e.,  $W_g(U, \Pi)$  around  $(0, 0)$ , while  $W_x(U, \Pi)$  moves around  $(2\Gamma, 0) = (1, 0)$ . When the two parts are summed up, the shape of the total Wigner function is not stable in time.

The Wigner function also provides a straightforward way of expanding a given quantum state expressed in terms of a Wigner function  $W(q, p)$ , be it pure or mixed, into any basis  $|\varphi_n\rangle$ . The probability of finding a state

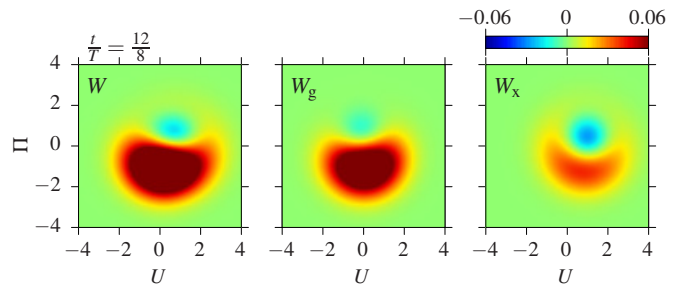


Figure 8. Snapshot at time  $t = 3T/4$  of the Wigner function (left), which can be separated into the Wigner function belonging to the ground state potential  $W_g(U, \Pi)$  (middle) and the one belonging to the exciton state potential  $W_x(U, \Pi)$  (right).

Table I. List of probabilities  $P_n^i$  finding Fock state  $|n\rangle$  in the subspace  $i = g, x$ .

$n$	$P_n^g$	$P_n^x$
0	0.46	0.09
1	0.25	0.19
2	0.005	$7 \times 10^{-4}$
3	$4 \times 10^{-5}$	$5 \times 10^{-6}$

$|\varphi_n\rangle$  is then given by<sup>33</sup>

$$P_n = \langle |\varphi_n\rangle \langle \varphi_n| \rangle = \pi \iint W_{\varphi_n}(q, p) W(q, p) dq dp \quad (23)$$

where  $W_{\varphi_n}(q, p)$  is the Wigner function representation of the projection operator  $|\varphi_n\rangle \langle \varphi_n|$ . Such an expansion can also be done separately for the Wigner functions in the two subspaces  $W_g(U, \Pi)$  and  $W_x(U, \Pi)$ . This allows us to expand the Wigner functions of the individual subspaces into the Fock states  $|n\rangle$  corresponding to the respective potential. The Wigner functions of the Fock states in the ground state subspace are given by

$$W_n^g(U, \Pi) = \frac{(-1)^n}{2\pi} e^{-\frac{1}{2}(U^2 + \Pi^2)} L_n(U^2 + \Pi^2)$$

with  $L_n$  being the Laguerre polynomials. For the Wigner functions  $W_n^x$  in the exciton system we take  $U \rightarrow U - 2\Gamma$ .

As an example we expand the Wigner functions from Fig. 8, where pronounced squeezing is visible. The probabilities obtained from this expansion are listed in Table I. Note that the sums of the probabilities in each subsystem reflect the electronic occupations. In our case, this means  $\sum_n P_n^g = \langle |g\rangle \langle g| \rangle = 1 - f \approx 0.715$  and  $\sum_n P_n^x = f \approx 0.285$ , as we have found in Fig. 5 a). Because the full state is normalized, it follows that  $\sum_n P_n^g + \sum_n P_n^x = 1$ . When looking at the actual numbers in Tab. I, we see that in each electronic subsystem only the first two Fock states, namely  $n = 0$  and  $n = 1$ , contribute significantly to the phonon state. As the listed probabilities  $P_1^g$ ,  $P_2^g$ ,  $P_1^x$  and  $P_2^x$  add up to almost 1, there are essentially no



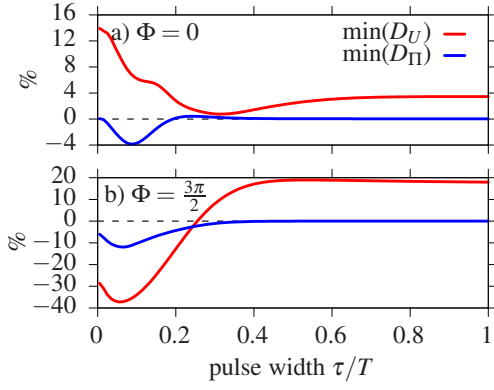


Figure 9. Minimal values of the fluctuations  $D_U$  and  $D_\Pi$  for a two pulse excitation with pulse areas  $\pi/2$  each and a delay of  $\Delta t = T/2$  as a function of the pulse width. a) Phase  $\Phi = 0$  and b) phase  $\Phi = 3\pi/2$ .

contributions from higher Fock states. The fact that the phonon state in each subsystem forms a superposition essentially of the form

$$c_0 |0\rangle + c_1 |1\rangle$$

is true for a wide range of pulse areas and durations. Recently it was shown that the photons emitted from QDs can be in a superposition of the lowest two Fock states  $|0\rangle$  and  $|1\rangle$ , and it was experimentally demonstrated that these photons exhibiting squeezing<sup>37</sup>. Though, the photons couple in a different way to the QD and are described within the Jaynes-Cummings model, this shows that squeezing in such a superposition occurs in a wider range of systems.

## 2. Two pulse excitation

For the two pulse excitation, we have already shown that squeezing can occur in the case of excitation by two ultra short pulses<sup>18,31</sup>. The strongest squeezing emerges, when the two pulses have a delay of  $\tau = T/2$  and a pulse area of  $\pi/2$  each. As we have seen, two pairs of phononic cat states build up, which for suitable coupling strengths (e.g.,  $\Gamma = 0.5$ ) give rise to squeezing. Another crucial pulse parameter is the phase difference  $\Phi$  between the two pulses. For a phase of  $\Phi = 0$  the state is not squeezed, while for  $\Phi = 3\pi/2$  the squeezing is maximal. This is in agreement with squeezing in cat states, which also depends crucially on the phase in the superposition state<sup>35</sup>. Let us briefly revisit the influence of the phase on the excitation: For the same phase, each pulse changes the occupations of the electronic states letting them perform a part of a Rabi rotation. When the phase difference is a multiple of  $\pi/2$ , the second pulse does not change the occupation of the states, but only influences the phase difference of the electronic states, which in turn modifies the phonon properties drastically<sup>31</sup>. In the following we will study how squeezing prevails using finite pulses.

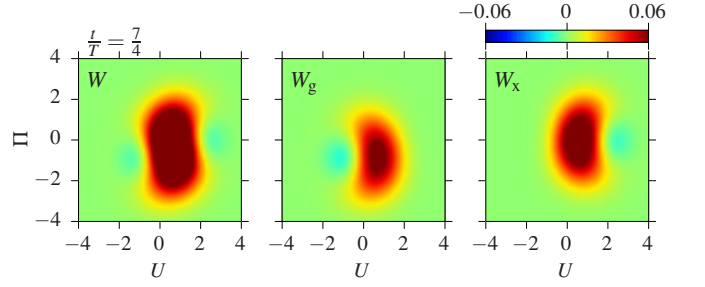


Figure 10. Snapshot at time  $t = 7T/4$  of the total Wigner function  $W(U, \Pi)$  (left) and the separation into  $W_g(U, \Pi)$  (middle) and  $W_x(U, \Pi)$  (right). The pulse width is  $\tau = 0.1T$  for two pulses with pulse area  $\pi/2$  each, a delay of  $T/2$  and a phase  $\Phi = 3\pi/2$ .

In Fig. 9 we show the minimum of the fluctuations  $D_U$  and  $D_\Pi$  for a two pulse excitation with pulse areas  $\pi/2$  each and a delay of  $\Delta t = T/2$  as a function of the pulse width for two different phases  $\Phi = 0$  and  $\Phi = 3\pi/2$ . For  $\Phi = 0$  we do not find any squeezing for ultra short pulses. For short pulses with  $\tau = 0.1T$  momentum squeezing occurs with a strength of about 5%, similar to the case of the one pulse excitation. For  $\tau > 0.2T$ , both fluctuations are larger than zero and we do not find squeezing. Interestingly, for  $0.6T < \tau < T$ , the fluctuations do not change as a function of pulse width anymore. Here, the two pulses already form a single pulse. Due to the phonon renormalization, the pulse area is slightly smaller than  $\pi$ . In this case a statistical mixture of two coherent states, one belonging to the ground state and one belonging to the exciton state, builds up leading to increased fluctuations in  $U$ , while the momentum fluctuations stay at zero. Note that these states are stationary and do not move in time.

For  $\Phi = 3\pi/2$  we already have squeezing of about 30% in the displacement and about 8% in the momentum at  $\tau = 0$ . If now the pulse width is taken to be finite, we see that the squeezing becomes even more pronounced with up to 40% in  $D_U$  at  $\tau = 0.1T$ . For larger pulse width  $\tau$  the squeezing in both displacement and momentum vanishes and for  $\tau > 0.6T$  also reaches a constant value almost independent of the pulse area.

It is interesting to note that also for a quantum well, i.e., for a system with a continuous electronic spectrum, a two-pulse excitation with finite pulses can lead to LO phonon squeezing under similar excitation conditions regarding the phase difference<sup>19</sup>.

The occurrence of squeezing for small pulse areas can be nicely seen in the Wigner function as displayed in Fig. 10, where we show a snapshot at time  $t = 7T/4$ , where the squeezing is maximal for the two pulse excitation, i.e.,  $D_U$  is minimal. When we separate the Wigner function into the ground state and exciton contribution with  $W(U, \Pi) = W_g(U, \Pi) + W_x(U, \Pi)$ , we see that already in the subspaces the Wigner functions are elongated in  $\Pi$ -direction with banana-like shapes oriented in

opposite directions. In addition, negative parts of the Wigner function are visible, indicating the non-classical character of the superposition of the cat states. When added up to the total Wigner function, as shown in the left part of Fig. 10, the Wigner function becomes squeezed.

#### IV. CONCLUSIONS

In summary, we have discussed the emergence of squeezed LO phonons by the optical manipulation of a QD. After reviewing the results for ultra short excitation, we have presented new results discussing the influence of

the pulse width on the creation of squeezed phonons. To this end, we have determined the solution of the equations of motion using a generating function formalism, from which the Wigner function can be calculated directly. For a single pulse, squeezing can be found if the pulse width is about  $0.05 - 0.5$  of the LO phonon period. In these cases superposition states are created leading to reduced fluctuations. In the case of a two-pulse excitation squeezing was already found for ultra-short pulses and we have shown that a strong squeezing prevails for extended pulses up to  $0.2T$ . Our results show that for extended pulses even stronger phonon squeezing can be observed, which brings the theoretical predictions one step closer to experimental realization.

- 
- <sup>1</sup> S. Volz, J. Ordonez-Miranda, A. Shchepetov, M. Prunila, J. Ahopelto, T. Pezeril, G. Vaudel, V. Gusev, P. Ruello, E.M. Weig, M. Schubert, M. Hettich, M. Grossman, T. Dekorsy, F. Alzina, B. Graczykowski, E. Chavez-Angel, J.S. Reparaz, M.R. Wagner, C.M. Sotomayor-Torres, S. Xiong, S. Neogi, D. Donadio, Eur. Phys. J. B **89**(1), 1 (2016)
  - <sup>2</sup> C. Brüggemann, A.V. Akimov, A.V. Scherbakov, M. Bombeck, C. Schneider, S. Höfling, A. Forchel, D.R. Yakovlev, M. Bayer, Nature Photon. **6**, 30 (2011)
  - <sup>3</sup> T. Czerniuk, C. Brüggemann, J. Tepper, S. Brodbeck, C. Schneider, M. Kamp, S. Höfling, B.A. Glavin, D.R. Yakovlev, A.V. Akimov, M. Bayer, Nature Comm. **5**, 4038 (2014)
  - <sup>4</sup> J.A.H. Stotz, R. Hey, P.V. Santos, K.H. Ploog, Nature Mat. **4**(8), 585 (2005)
  - <sup>5</sup> S. Völck, F.J.R. Schülein, F. Knall, D. Reuter, A.D. Wieck, T.A. Truong, H. Kim, P.M. Petroff, A. Wixforth, H.J. Krenner, Nano Lett. **10**(9), 3399 (2010)
  - <sup>6</sup> D.A. Fuhrmann, S.M. Thon, H. Kim, D. Bouwmeester, P.M. Petroff, A. Wixforth, H.J. Krenner, Nature Photon. **5**(10), 605 (2011)
  - <sup>7</sup> M. Weiß, J.B. Kinzel, F.J.R. Schülein, M. Heigl, D. Rudolph, S. Morkötter, M. Döblinger, M. Bichler, G. Abstreiter, J.J. Finley, G. Koblmüller, A. Wixforth, H.J. Krenner, Nano Lett. **14**(5), 2256 (2014)
  - <sup>8</sup> M.V. Gustafsson, T. Aref, A.F. Kockum, M.K. Ekström, G. Johansson, P. Delsing, Science **346**(6206), 207 (2014)
  - <sup>9</sup> M.L. Kerfoot, A.O. Govorov, C. Czarnocki, D. Lu, Y.N. Gad, A.S. Bracker, D. Gammon, M. Scheibner, Nature Comm. **5**, 3299 (2014)
  - <sup>10</sup> K.G. Nakamura, Y. Shikano, Y. Kayanuma, Phys. Rev. B **92**, 144304 (2015)
  - <sup>11</sup> J. Kabuss, A. Carmele, T. Brandes, A. Knorr, Phys. Rev. Lett. **109**(5), 054301 (2012)
  - <sup>12</sup> V.V. Dodonov, J. Opt. B: Quantum and Semiclassical Optics **4**, R1 (2002)
  - <sup>13</sup> E.S. Polzik, Nature **453**, 45 (2008)
  - <sup>14</sup> P.D. Drummond, Z. Ficek, *Quantum squeezing*, vol. 27 (Springer Science & Business Media, 2013)
  - <sup>15</sup> K. Goda, O. Miyakawa, E.E. Mikhailov, S. Saraf, R. Adhikari, K. McKenzie, R. Ward, S. Vass, A.J. Weinstein, N. Mavalvala, Nature Phys. **4**, 472 (2008)
  - <sup>16</sup> J. Janszky, A.V. Vinogradov, Phys. Rev. Lett. **64**, 2771 (1990)
  - <sup>17</sup> X. Hu, F. Nori, Phys. Rev. Lett. **76**, 2294 (1996)
  - <sup>18</sup> S. Sauer, J.M. Daniels, D.E. Reiter, T. Kuhn, A. Vagov, V.M. Axt, Phys. Rev. Lett. **105**, 157401 (2010)
  - <sup>19</sup> T. Papenkort, V.M. Axt, T. Kuhn, Phys. Rev. B **85**, 235317 (2012)
  - <sup>20</sup> E.S. Zijlstra, A. Kalitsov, T. Zier, M.E. Garcia, Phys. Rev. X **3**, 011005 (2013)
  - <sup>21</sup> G.A. Garrett, A.G. Rojo, A.K. Sood, J.F. Whitaker, R. Merlin, Science **275**, 1638 (1997)
  - <sup>22</sup> O.V. Misochko, Phys. Lett. A **269**, 97 (2000)
  - <sup>23</sup> S.L. Johnson, P. Beaud, E. Vorobeve, C.J. Milne, É.D. Murray, S. Fahy, G. Ingold, Phys. Rev. Lett. **102**, 175503 (2009)
  - <sup>24</sup> M. Esposito, K. Titimbo, K. Zimmermann, F. Giusti, F. Randi, D. Boschetto, F. Parmigiani, R. Floreanini, F. Benatti, D. Fausti, Nature Comm. **6**, 10249 (2015)
  - <sup>25</sup> A. Vagov, V.M. Axt, T. Kuhn, Phys. Rev. B **66**, 165312 (2002)
  - <sup>26</sup> V.M. Axt, T. Kuhn, A. Vagov, F.M. Peeters, Phys. Rev. B **72**, 125309 (2005)
  - <sup>27</sup> D. Wigger, D.E. Reiter, V.M. Axt, T. Kuhn, Phys. Rev. B **87**, 085301 (2013)
  - <sup>28</sup> D. Wigger, S. Lüker, D.E. Reiter, V.M. Axt, P. Machnikowski, T. Kuhn, J. Phys.: Condens. Matter **26**, 355802 (2014)
  - <sup>29</sup> D. Wigger, S. Lüker, V.M. Axt, D.E. Reiter, T. Kuhn, Photonics **2**(1), 214 (2015)
  - <sup>30</sup> T. Stauber, R. Zimmermann, H. Castella, Phys. Rev. B **62**, 7336 (2000)
  - <sup>31</sup> D.E. Reiter, D. Wigger, V.M. Axt, T. Kuhn, Phys. Rev. B **84**, 195327 (2011)
  - <sup>32</sup> V.M. Axt, M. Herbst, T. Kuhn, Superlattices and Microstructures **26**(2), 117 (1999)
  - <sup>33</sup> W.P. Schleich, *Quantum optics in phase space* (John Wiley & Sons, 2011)
  - <sup>34</sup> J. Janszky, P. Adam, A.V. Vinogradov, T. Kobayashi, Spectrochim. Acta Mol. Biomol. Spectrosc.y **48**(1), 31 (1992)
  - <sup>35</sup> C. Gerry, P. Knight, *Introductory quantum optics* (Cambridge University Press, 2005)
  - <sup>36</sup> S. Haroche, J.M. Raimond, *Exploring the quantum* (Oxford Univ. Press, 2006)

- <sup>37</sup> C.H.H. Schulte, J. Hansom, A.E. Jones, C. Matthiesen, C. Le Gall, M. Atatüre, *Nature* **525**, 222 (2015)